12

Combined solid-state closing switch for high-current pulse switching

© A.P. Orlov, P.I. Golyakov, Yu.V. Vlasov, P.B. Repin

Russian Federal Nuclear Center, All-Russia Research Institute of Experimental Physics,
607190 Sarov, Russia
e-mail: orlov@ntc.vniief.ru

Received May 25, 2023
Revised June 29, 2023
Accepted July 2, 2023

The results of studies of a solid-state closing switch for a high-current pulse switching are presented. The experiments were carried out on a laboratory facility with a capacitive energy storage run down a discharge circuit with electrical-explosive opening switch (EEOS) by a current pulse with an amplitude ~ 450 kA. The discharge circuit consists of two sections separated by a branch with a solid-state closing switch. A metal foil of the EEOS can be located in an interelectrode gap of the closing switch. The operation of the EEOS leads to a breakdown of the insulation of the closing switch, as a result of which an effective shunting of the section of the discharge circuit containing the EEOS occurs. The developed combined solid-state closing switch in the future is capable of providing multi-channel switching of a high-current pulse to the load synchronously with the EEOS operation.

Keywords: current switching, electrical-explosive opening switch, solid-state closing switch, closing time of a switch, final resistance of a switch.

DOI: 10.61011/TP.2023.09.57368.136-23

Introduction

The phenomenon known in physics as the electrical explosion of a conductor is a sudden change in its physical state under the action of a pulsed electric current of high density, leading to the disappearance of metallic electrical conductivity and accompanied by the effects characteristic of an electrical explosion —radiation and the formation of shock waves [1]. The principle of electrical explosion of a conductor is the basis for the operation of electrical explosive current disconnectors (EEOS). Compared to other types of disconnectors, the EECD is characterized by its simple construction and low intrinsic inductance. Its working fluid is a foil or wires arranged in a dielectric (arc-quenching) medium. EEOSs have found application in the creation of powerful power sources based on explosive magnetic generators for powering liner ponderomotor units [2], as well as for the formation of high-voltage pulses in high-impedance loads [3,4]. Under determined conditions, due to fast resistance growth and low inductance, EEOS can be used as a second aggravation stage and form mega ampere current pulses with an $\sim 0.1\,\mu$s [5] front. The load connection in such devices is usually made using a solid-state or gas-filled closing switch (CS) [6]. One possible design of a multichannel solid-state arrester for nanosecond switching of mega-ampere currents is proposed in [7].

The advantages of solid-state CS include their compactness, manufacturability, and ability to hold high voltages for long periods of time. But there are also disadvantages, such as relatively long response time and high final resistance and inductance values, which result in a current pulse with a longer edge and much smaller amplitude than required in the load circuit. High final values of resistance and inductance of CS are caused by the formation of a limited number of breakdown channels in the volume of the CS insulator. Thus, it is known from experiments [6] that, as a rule, only one channel is formed in such devices when a voltage pulse with a rising rate $dU/dt < 10^{11}$ V/s is applied to the dielectric. For simultaneous (during $\sim 10^{-9}$ s) formation of multiple breakdown channels, pulses with a steep front $dU/dt \geq 10^{12}$ V/s must be applied to the dielectric. However, this voltage rise rate requirement is difficult to achieve in most cases of practical interest. It is possible to provide a multichannel mode of operation of the CS by using an external control high-voltage pulse, but in this case, taking into account possible deviations of amplitude and time parameters of the inductive accumulator and EEOS from the set values, the moment of load connection, determined by the predetermined moment of the control signal supply, may differ significantly from the optimal one from the point of view of the EEOS operation. Also to the disadvantages of solid-state CS should be attributed instability of the moment of its operation, due to the scattering of values of the breakdown voltage of the dielectric, which, in turn, can lead to variations from experience to experience rise time and amplitude of the current pulse in the load. For example, at breakdown of various industrial samples of lavsan insulator there is a 30% variation of values of breakdown voltage [8] due to the presence of microdefects, inhomogeneities and extraneous micro-inclusions affecting its electrical strength.

This paper presents the results of research on the development of a solid-state CS design capable of providing both multichannel switching of a high-current pulse into the load under conditions when $dU/dt < 10^{12}$ V/s, and synchronization of the moment of load connection with

the operation of EEOS. The fulfilment of the last condition is necessary in case of deviations of the operation of the inductive accumulator and EEOS from the design mode, which is especially important in expensive experiments with explosive magnetic generators.

The studies were carried out on a laboratory electrophysical setup at a current with amplitude ~ 450 kA, increasing over time $\sim 1\,\mu$s.

1. Description of the installation and features of its operation

The equivalent circuit diagram of the experimental setup for investigating the operation of the closing key is shown in Fig. 1, *a*). The unit consists of: a capacitor bank *1* of capacitance $7.2\,\mu$F with charging voltage 83 kV; inductance *2* (70 nH), resistance *3* (20 m Ω) and capacitance *4* (10 nF) of the cable lines that carry electrical energy from the capacitor bank to the discharge circuit; inductances *5* (20 nH) and *6* (24 nH) in the discharge circuit; variable resistance EEOS *7*; variable resistance CS *8*.

During the operation of the device the current from the source *1* through inductances *5* and *6* is led to the EEOS consisting of an aluminium foil, part of which can be located in the gap of the CS between the potential electrode and the film insulator (combined version of the CS, Fig. 1,*b*). As a result of current flow, the foil first heats up, then melts and begins to vaporize, which causes a sharp increase in the resistance of the EEOS and an increase in the voltage on the CS. When the CS is activated, a section of the

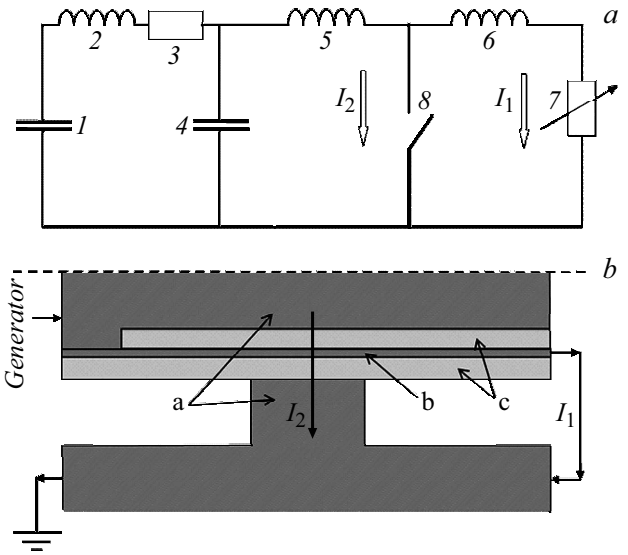

Figure 1. *a* — The equivalent electrical circuit of the CS research setup. *1* — capacitor bank, *2–4* — inductance, resistance and capacitance of the supply lines, *5, 6* — inductance of the discharge circuit sections, *7* — resistance of EEOS, *8* — shorting key; *b* — diagram of the combined shorting switch consisting of electrodes (*a*), EEOS foil section (*b*) and film insulators (*c*). I_1 — current through the EEOS, I_2 — current through the closing key.

discharge circuit consisting of the inductance *6* and EEOS *7* is shunted.

In difference from the variant of CS, in which the foil in its gap is absent, in the combined CS along with the increase of voltage on it due to the foil electroexplosion there are accompanying factors — shock wave and electromagnetic radiation [1], causing multi-channel and azimuthally homogeneous CS breakdown [9].

The thickness of the EEOS foil is selected in a design-experimental way, so that its electric explosion occurs near the moment of current maximum in the discharge circuit. The thickness of the CS insulator must provide the necessary electrical strength and prevent premature tripping. In the present work, results are presented for a design variant with an optimum EEOS working fluid in the form of a single layer of aluminium foil of thickness $9\,\mu$m, width 116 mm, length 60 mm and CS insulators of total thickness $160\,\mu$m.

2. The computational model of the EEOS and latching key

To calculate the time variation of resistance R_f of the EEOS foil due to its Joule heating when current I_1 flows, the differential equation is used

$$de/dt = I_1(t)^2 R_f(e)/m,$$

$$m = \rho_0 Sl, \quad R_f(e) = R_0\eta(e), \quad R_0 = l/(\sigma_0 S),$$

where $e(t)$ — the thermal component of the internal energy of a unit mass of foil, counted from the initial value at normal conditions ($e(0) = 0$); $S = \pi D\delta$ — the cross-sectional area of the foil; R_0, σ_0, m, ρ_0, l, δ, D — initial resistance, conductivity coefficient, total mass, density, length, thickness and diameter of the foil arrangement. The dependence $\eta(e) = R_f/R_0$ in the range $0 < e < e_{\text{burst}}$, where e_{urst} — value of the specific thermal energy of the foil at its complete evaporation (electric explosion), is tabular and can be taken, for example, from the works [1,10,11]. In accordance with the data given in [11,12], the computational model assumes that in the energy range $e_{\text{burst}} < e(t) < 2e_{\text{burst}}$ the resistance of the EEOS is maximum and equal to $R_f(e_{\text{burst}})$. If at the final stage of commutation there is further heating of foil electrical explosion products by the flowing current, it leads to the transition of the vaporized substance to the plasma state, accompanied by a drop in the resulting electrical resistance from thermal energy. In the computational model, this process is described by the Spitzer conductivity ($\sigma \propto T^{3/2}$), which is characteristic of the plasma state of matter, and it is assumed that in the case of $e(t) > 2e_{\text{burst}}$ the resistance of the EEOS falls in accordance with $R_f(e) = R_0\eta(e_{\text{burst}})/\big(e/(2e_{\text{burst}})\big)^{3/2}$.

According to the existing theoretical concepts, the electrical breakdown of a solid-state CS insulator has two successive stages — the dielectric loss of electrical strength and its destruction [13]. If the first stage of breakdown begins

when the breakdown electric field strength E_{br} is reached in its volume, then during the second stage the effective ohmic resistance of CS decreases from a large initial value to some final value depending on the number of breakdown channels formed at the first stage. Taking into account the described phenomena in the used calculation model, the two-stage operation of the investigated solid-state CS with multilayer lavsan insulation ($E_{\text{br}} = 140-180$ kV/mm [8]) of total thickness $\Delta = 0.16$ mm was numerically modelled by time-variable resistance as $R_{cs}(t) = 1\,\text{M}\Omega$ at $t < t_{\text{br}}$ and

$$R_{cs}(t) = R_{close} + (R_{cs}(t_{\text{br}}) - R_{close}) \exp\left[-(t - t_{\text{br}})/t_{close}\right]$$

at $t \geq t_{\text{br}}$, where the time t_{br} corresponds to the moment when the breakdown voltage $U_{\text{br}} = E_{\text{br}}\Delta \approx 22-29$ kV reaches the CS. Two free parameters (characteristic duration of the CS insulation failure process t_{close} and its final ohmic resistance R_{close}) in the computational model are varied for the best agreement with the experimental results.

3. Experimental results and discussion

Fig. 2 shows experimental oscillograms and calculated dependences of currents in the absence of foil in the CS gap. This experimental configuration made it possible to exclude the impact on the CS operation of the mechanical action of the shock wave, as well as other factors accompanying the electric explosion. The breakdown of the CS insulator in this case is ensured only by the overvoltage developed during the operation of EEOS, when the voltage $U > U_{\text{br}}$ is realized on the CS insulator. The computational modelling reproduces the experimental results well for the following CS parameters: $t_{close} = 0.003\,\mu$s, $R_{close} = 0.01\,\Omega$. Fig. 3 shows the experimental results in the case of foil placement in the CS gap and the results of computational modelling for the following CS parameters: $t_{close} = 0.003\,\mu$s, $R_{close} = 0.002\,\Omega$.

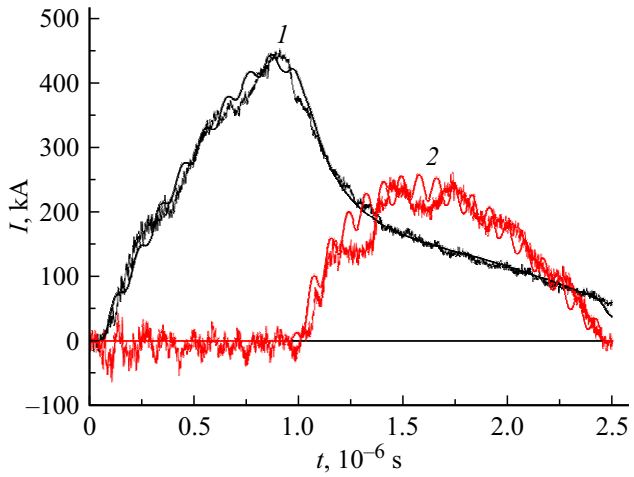

Figure 2. Oscillograms (bold lines) and calculated (thin lines) dependences of currents when there is no foil between the CS electrodes. *1* — current through the EEOS, *2* — current through the closing key.

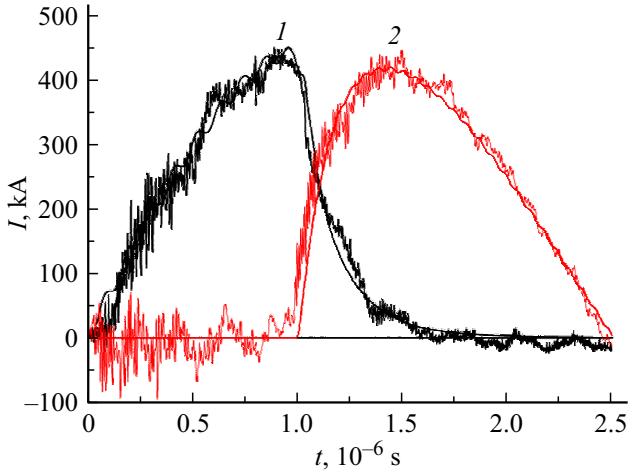

Figure 3. Oscillograms (bold lines) and calculated (thin lines) dependences of currents in the presence of foil between the CS electrodes. *1* — current through the EEOS, *2* — current through the closing key.

Figure 4. Photographs of the electrode surface. *a* — experiment without the EEOS foil in the gap of the gating, *b* — experiment with the EEOS foil in the CS gap

.

The comparison of experimental currents in Fig. 2 and 3 shows that in the absence of the EEOS foil in the CS gap, the moment of commutation onset remained practically unchanged, but there was a noticeable (by 1.8 times) decrease in the amplitude and delay of the front of the current pulse through the CS, which indicates the deterioration of commutation parameters. The computational modelling of the experimental results shows that the duration t_{close} of the gating operation does not change, and its final

resistance R_{close} without foil in the gap increases by 5 times in comparison with the case of the presence of the foil section of the EEOS in the CS gap. This result is due to the azimuthally uniform current distribution over the entire cylindrical surface of the CS at the initial presence of the EEOS foil in the gap, in contrast to the variant when it is absent — in this case, as a rule, a single-channel breakdown mode is realized. As an illustration of the above, photographs of the electrodes after the corresponding experiments are shown in Fig. 4.

4. Conclusion

1) The experiments carried out in two configurations of axially symmetric CS with lavsan insulation demonstrated different switching properties: in the case of the presence of the EEOS foil in the gap of the gear, a current pulse with an amplitude of 410 kA and a rise time of 400 ns was passed through it against, respectively, 240 kA and 550 ns in the case of the absence of the foil in the CS gap.

2) The computational modelling has shown that the improvement of switching properties is due to the implementation of a lower value of the final resistance of the CS (approximately 5 times) in the case of the combined with EEOS variant of its design. Photographs of the electrodes after the experiments also confirm the azimuthally uniform current distribution over the entire cylindrical surface of the CS in the presence of foil in the gap, in contrast to the variant when there is no foil in the gap.

Thus, the experimental results indicate that the factors accompanying the electric explosion of the EEOS foil (shock wave and electromagnetic radiation) actively participate in the breakdown of the CS insulation along with the overvoltage developed during the EEOS operation. The above factors ensure effective destruction of the insulator throughout the CS annular gap, resulting in its lower ohmic resistance in the closed state. The obtained experimental results and computational model can be used in the development of new versions of experiments on switching megaampere current pulses with the help of a solid-state combined CS when powered from more powerful, including explosive-magnetic, current generators. In particular, at the electrophysical installation at the maximum current level of 800 kA the developed combined EQ allowed to pass a current pulse with amplitude ≈ 670 kA and rise time of 300 ns formed with the help of EEOS.

Conflict of interest

The authors declare that they have no conflict of interest.

References

[1] V.A. Burtsev, N.V. Kalinin, A.V. Luchinskiy, *Elektricheskiy vzryv provodnikov i ego primenenie v elektrofizicheskikh ustanovkakh* (Energoatomizdat, M., 1990) (in Russian).

[2] A.M. Buyko, V.A. Vasyukov, Yu.N. Gorbachev, B.T. Yegorychev, V.A. Ivanov, V.B. Kudelkin, A.I. Kuzyaev, A.A. Kulagin, B.I. Leukhin, I.V. Morozov, V.N. Mokhov, V.V. Pavliy, S.V. Pak, A.A. Petrukhin, N.M. Sabayev, A.N. Skobelev, V.V. Chernyshev, V.K. Chernyshev, V.B. Yakubov, B.G. Anderson, W.L. Atchison, D.A. Clark, R.J. Faehl, I.R. Lindemuth, R.E. Reinovsky, G. Rodriguez, J.L. Stokes, L.J. Tabaka. In: *Megagauss-9*, ed. by V.D. Selemir, L.N. Plyashkevich (VNIIEF, Sarov, 2004), p. 752.

[3] V.A. Demidov, A.S. Boriskin, N.V. Stepanov, I.V. Konovalov, S.A. Kazakov, K.V. Shibalko, Yu.V. Vlasov, V.A. Yanenko, I.V. Rozhnov, S.N. Golosov, E.V. Shapovalov, A.S. Shuvalov. In: *Megagauss X*, ed. by M. von Ortenberg (Humboldt University, Berlin, 2005), p. 94.

[4] A.S. Kravchenko, A.S. Boriskin, Yu.V. Vilkov, V.D. Selemir, E.M. Dimant, A.S. Yuryzhev, D.I. Zenkov, A.A. Tkachuk, E.N. Kirshanova, M.B. Kozlov. Instruments and Experimental Techniques, **43**—,(2), 213 (2000).

[5] A.A. Bazanov, E.I. Bochkov, S.G. Garanin, P.V. Duday, A.A. Zimenkov, A.V. Ivanovskiy, K.N. Klimushkin, V.M. Komarov, A.I. Krayev, V.B. Kudel'kin, V.I. Mamyshev, S.M. Polyushko, Z.S. Tsibikov, E.V. Shapovalov. Dokl. Phys., **64** (12), 443 (2019).

[6] G.A. Mesyats. *Impulsnaya energetika i elektronika* (Nauka, M., 2004) (in Russian)

[7] E.A. Galanova, Y.N. Dolin, A.V. Ivanovsky, A.E. Kalinichev, G.V. Karpov, S.S. Lomtev, A.G. Merzlov, V.N. Nudikov, D.S. Prokhorov, E.A. Salatov, A.N. Turov, A.A. Shatalin. Doklady RAN. Fizika, tekhnicheskie nauki, **506** (2), 34 (2022). DOI: 10.31857/S2686740022070045

[8] I.S. Grigoryev, E.Z. Mejlikhov (red.). *Fizicheskie velichiny, Spravochnik.* (Energoatomizdat, M., 1991) (in Russian).

[9] P.I. Golyakov, P.B. Repin, A.G. Repiev, A.P. Orlov. Patent RU 2766434, H01H 39/00, (2022)

[10] T.J. Tucker, R.P. Toth. *Sandia National Laboratory Report.* SAND-75-0041 (USA, SNL, 1975)

[11] H. Knoepfel. *Pulsed High Magnetic Fields* (North-Holland, Amsterdam-London, 1970)

[12] Y.V. Vlasov, V.A. Demidov, V.I. Skokov. In: *Impul'snyye tekhnologii megagauss i megaamper i ikh primeneniye*, ed. by V.K. Chernyshev, V.D. Selemir, L.N. Plyashkevich (Sarov, VNIIEF, 1997), p. 372.

[13] G.A. Vorobiev, Yu.P. Pokholkov, Yu.D. Korolev, V.I. Merkulov. *Fizika dielektrikov* (*oblast' silnykh polei*) (Tomsk, TPU 2003) (in Russian).

Translated by Y.Deineka